TECHNICAL REPORT
NATICK/TR-22/032

AD _____

TORSO PLATE BACKING EVALUATION

by
Melissa J. Roth

August 2022

Final Report
October 2018 – October 2020

Approved for public release; distribution is unlimited.

U.S. Army Combat Capabilities Development Command Soldier Center
Natick, Massachusetts 01760-5000

DISCLAIMERS

The findings contained in this report are not to be construed as an official Department of the Army position unless so designated by other authorized documents.

Citation of trade names in this report does not constitute an official endorsement or approval of the use of such items.

DESTRUCTION NOTICE

For Classified Documents:

Follow the procedures in DoD 5200.22-M, Industrial Security Manual, Section II-19 or DoD 5200.1-R, Information Security Program Regulation, Chapter IX.

For Unclassified/Limited Distribution Documents:

Destroy by any method that prevents disclosure of contents or reconstruction of the document.

REPORT DOCUMENTATION PAGE

Form Approved
OMB No. 0704-0188

PLEASE DO NOT RETURN YOUR FORM TO THE ABOVE ADDRESS.

1. REPORT DATE *(DD-MM-YYYY)*	2. REPORT TYPE	3. DATES COVERED *(From - To)*
4-08-2022	Final	1 Oct 2018 – 31 Oct 2020

4. TITLE AND SUBTITLE

TORSO PLATE BACKING EVALUATION

5a. CONTRACT NUMBER

5b. GRANT NUMBER

5c. PROGRAM ELEMENT NUMBER

6. AUTHOR(S)

Melissa J. Roth

5d. PROJECT NUMBER
19-225

5e. TASK NUMBER

5f. WORK UNIT NUMBER

7. PERFORMING ORGANIZATION NAME(S) AND ADDRESS(ES)
U.S. Army Combat Capabilities Development Command Soldier Center
ATTN: FCDD-SCD-PMB
10 General Greene Avenue, Natick, MA 01760-5000

8. PERFORMING ORGANIZATION REPORT NUMBER

NATICK/TR-22/032

9. SPONSORING / MONITORING AGENCY NAME(S) AND ADDRESS(ES)

10. SPONSOR/MONITOR'S ACRONYM(S)

11. SPONSOR/MONITOR'S REPORT NUMBER(S)

12. DISTRIBUTION / AVAILABILITY STATEMENT

Approved for public release; distribution is unlimited.

13. SUPPLEMENTARY NOTES

14. ABSTRACT

The work described herein was performed by the Combat Capabilities Development Command (DEVCOM) Soldier Center using Core S&T funds during the period October 2018 – October 2020 in support of the Blast and Ballistics Community of Practice Torso and Extremity Protection Goal of understanding protective mechanisms and materials of ballistic armor. This effort focused on relating mechanical properties of ultra-high molecular weight polyethylene (UHMWPE) composites to ballistic performance. Results showed that flexural strength was the strongest predictor of Threat E V_{50} performance.

15. SUBJECT TERMS

V50	THREAT E	SHEAR STRENGTH	TEST AND EVALUATION
TORSO	PROTECTION	TENSILE STRENGTH	COMPOSITE MATERIALS
ARMOR	BODY ARMOR	CERAMIC MATERIALS	BALLISTIC PERFORMANCE
PLATES	RIFLE THREAT	FLEXURAL STRENGTH	MECHANICAL PROPERTIES
UHMWPE	AREAL DENSITY	UHMWPE COMPOSITES	SMALL ARMS PROTECTION
DYNEEMA	BALLISTIC TESTS	BALLISTIC PROTECTION	PERFORMANCE(ENGINEERING)

ULTRA-HIGH MOLECULAR WEIGHT POLYETHYLENE
UHMWPE(ULTRA HIGH MOLECULAR WEIGHT POLYETHYLENE)

16. SECURITY CLASSIFICATION OF:			17. LIMITATION OF ABSTRACT	18. NUMBER OF PAGES	19a. NAME OF RESPONSIBLE PERSON
a. REPORT	b. ABSTRACT	c. THIS PAGE			Melissa Roth
U	U	U	SAR	32	19b. TELEPHONE NUMBER *(include area code)* (508) 206-3040

Standard Form 298 (Rev. 8-98)
Prescribed by ANSI Std. Z39.18

This page is intentionally blank.

Table of Contents

List of Figures

List of Tables

Preface

The work reported herein was performed by the U.S. Army Combat Capabilities Development Command Soldier Center (DEVCOM SC) in support of the Blast and Ballistics Community of Practice Torso and Extremity Protection Goal of understanding protective mechanisms and materials of ballistic armor. Work was performed during the period from October 2018 – October 2020 using Core Science and Technology (S&T) funds under the project Torso Plate Backing Evaluation (19-225). Recent developments in ultra-high molecular weight polyethylene (UHMWPE) composite materials from industry have shown good performance in lightweight rifle helmets but have not been thoroughly explored in hard armor systems. The goal of this study was to evaluate the composite properties in relation to their ballistic performance in torso plates in order to achieve lighter weight torso protection.

Acknowledgements

The author would like to thank Robert DiLalla, Dr. David Colanto, Sean Smith, Damian Kubiak, and Jason Parker for their assistance and guidance on this project.

TORSO PLATE BACKING STUDY

1 Introduction

The work reported herein was performed by the U.S. Army Combat Capabilities Development Command Soldier Center (DEVCOM SC) in support of the Blast and Ballistics Community of Practice Torso and Extremity Protection Goal of understanding protective mechanisms and materials of ballistic armor. Work was performed during the period from October 2018 – October 2020.

Ultra-high molecular weight polyethylene (UHMWPE) composites are a mass efficient ballistic protection material. The long polyethylene (PE) chains provide good energy transfer throughout the composite while features such as void size, resin type and content, stiffness, and shear strength may also affect performance. The goal of this study was to understand how the mechanical properties of the composites affect the ballistic performance. The design-build-test method of testing composites against ballistic threats can be a timely and expensive process, and thus having a relationship between lab-scale mechanical tests and ballistic limit (V_{50}) could help aid in the design of armor in a more efficient manner.

The first step was to explore the relationship between mechanical properties and processing conditions for a variety of UHMWPE composites so that once a relationship between these properties and V_{50} is established, the proper processing conditions can be selected to optimize performance. The temperature and pressure at which the laminates are consolidated will affect polymer degradation, resin flow, fiber movement, and interfacial properties.

The next phase of this effort included testing the composites in conjunction with a ceramic strike face against Threat E. These data were compared to the mechanical properties to see if relationships between mechanical properties and ballistic performance exist.

2 Materials

2.1 Equipment

Table 1 provides a list of equipment used to make samples and perform lab testing at DEVCOM SC.

Table 1 - Production and test equipment used

Equipment	Manufacturer	Specifications
Gas gun	Physics Applications Inc.	Compressed helium gas gun with 2.74 m (9 ft) smooth-bore barrels, Sydor light screens for velocity measurements
Universal test machine	Instron®	Model 5969
Lab scale	Sartorius	Model LA3200D
352 ton hydraulic press	Icon	20” diameter ram

2.2 Materials

DSM and Honeywell composites are comprised of unidirectional UHMWPE fibers prepregnated with a resin and stacked in a [0°/90°] or $[0°/90°]_2$ orientation depending on the material. Materials used for this study are listed in Table 2.

Table 2 - UHMWPE composite materials

UHMWPE Composite Material	Manufacturer	Resin Type	Cross-ply Construction	Areal Density Kg/m^2 (lb/ft^2)
Dyneema® HB210	DSM	Polyurethane	$[0°/90°]_2$	0.136 (0.0278)
Dyneema® HB212	DSM	Rubber	$[0°/90°]_2$	0.136 (0.0278)
Dyneema® HB311	DSM	Polyurethane	$[0°/90°]_2$	0.104 (0.0213)
Dyneema® HB460	DSM	Unknown	[0°/90°]	0.0736 (0.0151)
Dyneema® X293	DSM	Unknown	[0°/90°]	0.104 (0.0213)
Spectra Shield® 5143	Honeywell	Rubber	$[0°/90°]_2$	0.163 (0.0334)
Spectra Shield® 5231	Honeywell	Polyurethane	$[0°/90°]_2$	0.167 (0.0342)

SikaFlex 252 adhesive, UltraSic™ SC-30 ceramics, and a Cordura® wrap were used to make the flat samples for Threat E ballistic tests. Materials used are outlined in Table 3.

Table 3 - Materials and projectiles used for ballistic tests

Materials	Manufacturer	Specifications
SikaFlex 252	Sika AG	Polyurethane adhesive
UltraSic™ SC-30 ceramic	CoorsTek	10.2 cm x 10.2 cm x 0.8 cm (4 in x 4 in x 0.315 in) flat tiles, density 3.15 g/cm^3 (0.114 lb/in^3), areal density 2.52 g/cm^2 (5.17 lb/ft^2)
Cordura® adhesive wrap	Cordura®	Woven nylon plate covering
1.10 g (17 gr) fragment simulating projectiles (FSP)	PTI Machine	.15 cal, T37 shape, hardened steel
2.85 g (44 gr) FSP	PTI Machine	.22 cal, T37 shape, hardened steel
Threat E Projectiles	Contra Threat	

3 Methods

Composites were pressed at multiple temperature and pressure conditions as needed for an array of mechanical and ballistic testing.

3.1 Sample Preparation

UHMWPE prepreg sheets were consolidated under heat and pressure to create a flat panel composite. The consolidation pressures and temperatures outlined in the test matrix in Table 4 were selected based on manufacturer-recommended processing conditions plus a high and low value. The high pressure was limited by the maximum output of the 392 ton press. A full list of material and processing conditions matrix can be found in Appendix A.

Table 4 - Processing condition test matrix

Temperature °C (°F)	Pressure MPa (psi)
120 (248)	20.7 (3000)
135 (275)	20.7 (3000)
146 (295)	20.7 (3000)
135 (275)	2.76 (400)
135 (275)	24.0 (3480)

To consolidate, sheets of composites cut to 38 cm x 38 cm (15 in x 15 in) were arranged in a 0°/90° orientation and placed between sheets of fiberglass-reinforced Teflon® release paper. These layups were then placed between two aluminum caul plates. This was then placed in between the platens of the pre-heated press until just touching in order to heat up for 10 min. Next, pressure was applied for 20 min. The composites were then cooled to room temperature while under pressure.

Single sheets were pressed and heat treated for tensile tests. Panels with an areal density of 4.9 kg/m^2 (1 lb/ft^2) were consolidated for density, micro computed tomography (micro CT), flexural testing, 1.1 g (17 gr) FSP V_{50}, and Threat E V_{50} testing. Panels with an areal density of 7.3 kg/m^2 (1.5 lb/ft^2) were consolidated for 2.85 g (44 gr) FSP testing. For hybrid panels made of more than one material, the sheets were stacked to achieve a 50% weight areal density of each material and were consolidated together under heat and pressure as described above.

3.2 Density

Density was measured using the Archimedes method according to ASTM D792-13 [1]. The purpose was to explore how processing conditions affect void formation and recrystallization. A lower density indicates a higher void content or that during cooling the PE and resin have formed less dense amorphous regions and have lost crystalline structure. The formation of voids is undesirable because it weakens the matrix and does not allow for efficient energy dissipation. It also induces localized stress concentration.

Samples were cut from flat plates using a band saw to roughly 38 mm x 18 mm (1.5 in x 0.7 in). A bowl of water at room temperature was placed underneath the scale so that the wet mass of the specimens could be measured. Samples were suspended from a metal wire sample holder, which

was connected to a metal sinker. The wire was looped around a hook on the underside of the scale for measuring mass.

First, the mass of the specimen in air (*a*) was measured. The specimen was then placed in the sample holder. The sample, sample holder, and sinker were suspended from the underside of the scale such that the sample and sinker were fully submerged in the water. This mass (*b*) was recorded. Next, the sample was removed and the wet mass of the sample holder and sinker (*w*) was recorded.

For each specimen, the specific gravity was calculated using the following equation:

$$sp\ gr\frac{23}{23}℃ = a/(a + w - b) \qquad \text{Eq 1}$$

The density of the plastic was then calculated using Eq. 2, where ρ is the density of the water at the measured temperature.

$$D^{23C}\left(\frac{kg}{m^2}\right) = sp\ gr\frac{23}{23}℃ \times \rho \qquad \text{Eq 2}$$

Five specimens were measured for each sample.

3.3 Micro CT

Samples were sent out for micro CT imaging at NTS Chesapeake. Micro CT can show defects within the laminates and calculate the void ratio caused by the presence of pores and delamination. The defect volume ratio is the ratio of porosity volume to total volume expressed as a percentage, which can be correlated with specific gravity. Pores in the laminate structure lead to localized stresses, which can have deleterious effects on the mechanical properties of the composite.

3.4 Tensile Strength

Tensile test specimens were prepared by cutting a single heat- and pressure-treated lamina to 230 mm (9 in) long by 13 mm (0.5 in) wide. Materials X293 and HB460 consist of a single [0°/90°] ply while all others consist of 2 [0°/90°] plies. An Instron 5963 universal test machine with 5 kN load cell and smooth steel clamping actuators was used to measure load vs extension. Pieces of paper were folded over the tops of the strips to prevent slipping before clamping at 620 kPa (90 psi). The gauge length was set to 10 cm (3.9”) and the top crosshead was moved up at a rate of 50 cm/min (15.75 in/min) until specimen failure. A minimum of 20 specimens were tested for each sample.

3.5 Short Beam Shear Strength

The purpose of the three-point bend test was to measure shear strength of the composites and how it varies with processing conditions. The shear strength can be correlated with the inter-ply strength of the laminates. The type of failure mechanism observed may also offer insight as to how resin and interlaminar properties affect ballistic performance. Laminates were cut to a length-to-thickness ratio of 6:1 and a width-to-thickness ratio of 2:1 as specified by ASTM D2344 [2]. An Instron universal test machine was equipped with a flex fixture and short beam shear head as shown in Figure 2. The span of the flex fixture was set such that the span-to-thickness ratio was 4:1.

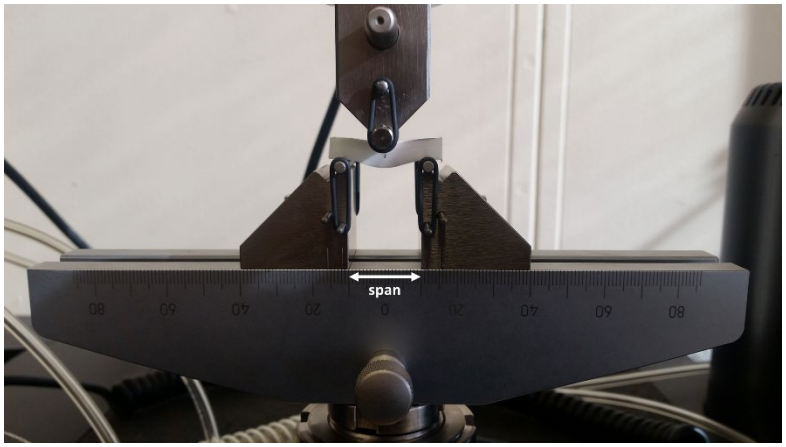

Figure 1 - The Instron flex fixture with short beam shear head

The crosshead to which the short beam shear head was attached was moved downwards at a rate of 1 mm/min (0.04 in/min) until the load dropped by 30%, signaling the end of the test. For each specimen, the load as a function of displacement was measured. The short beam strength was calculated using Eq. 3, where P_m is the maximum load recorded, b is the specimen width, and h is the specimen thickness.

$$F^{sbs} = 0.75 \times \frac{P_m}{b \times h} \quad \text{Eq. 3}$$

Specimens were observed for failure mechanisms. Delamination between plies of material indicates interlaminar shear failure, while the absence of these would indicate inelastic deformation. Ten specimens were tested for each sample.

3.6 Flexural Strength

Flexural stiffness was measured using a four-point bend method because flexural stiffness of the composites has been shown to affect ceramic performance in torso plates [3]. For four point bending, the maximum fiber stress is distributed evenly between the loading noses of the top beam, as opposed to three-point bending measured in Section 3.2.4, where the maximum load is immediately under the single nose. The peak stress is along an extended region of the sample.

Composites roughly 6 mm (0.24 in) in thickness were cut to 90 mm (3.5 in) in length and 10 mm (0.39 in) wide. They were centered on top of a four-point bend fixture for the Instron universal test machine with a base span of 80 mm (3.1 in) and load span of 40 mm (1.6 in) as specified by Procedure B of ASTM 7264 [4]. The load span to which the load span was affixed was brought down on the sample at a rate of 0.018 mm/s (0.0007 in/s) to obtain a strain rate of 10^{-4} s^{-1}. The flexure stress as a function of extension was measured. Flexural strength of the composites was calculated using Eq. 4, where P is the break force of maximum force, L is the specimen length, b is the specimen width, and d is the specimen thickness.

$$S = \frac{3PL}{4bd^2} \quad \text{Eq. 4}$$

A minimum of 10 specimens were tested per sample.

3.7 Ballistic Tests

V_{50} values were obtained on flat panels for 1.1 g (17 gr) FSPs, 2.85 g (44 gr) FSPs, and Threat E. The 4.9 kg/m^2 (1 lb/ft^2) plates were evaluated against 17 gr FSPs and 7.3 kg/m^2 (1.5 lb/ft^2) plates were evaluated against 44 gr FSPs. The FSPs were tested at CCDC SC using a gas gun and Threat E ballistic tests were conducted at NTS Chesapeake (Belcamp, MD).

V_{50} values were calculated by averaging the three lowest complete penetration velocities and the three highest partial penetration velocities.

4 Results and Discussion

Analysis of means was used to determine if there were any statistically significant differences in properties processed at different conditions. A Tukey-Kramer test was used for those materials with three sample sets and a pooled t test was used for materials with two sample sets. Comparisons that had $p<0.05$ were considered statistically significant.

4.1 Density

Figures 3 and 4 show the changes in specific gravity as functions of temperature and pressure, respectively.

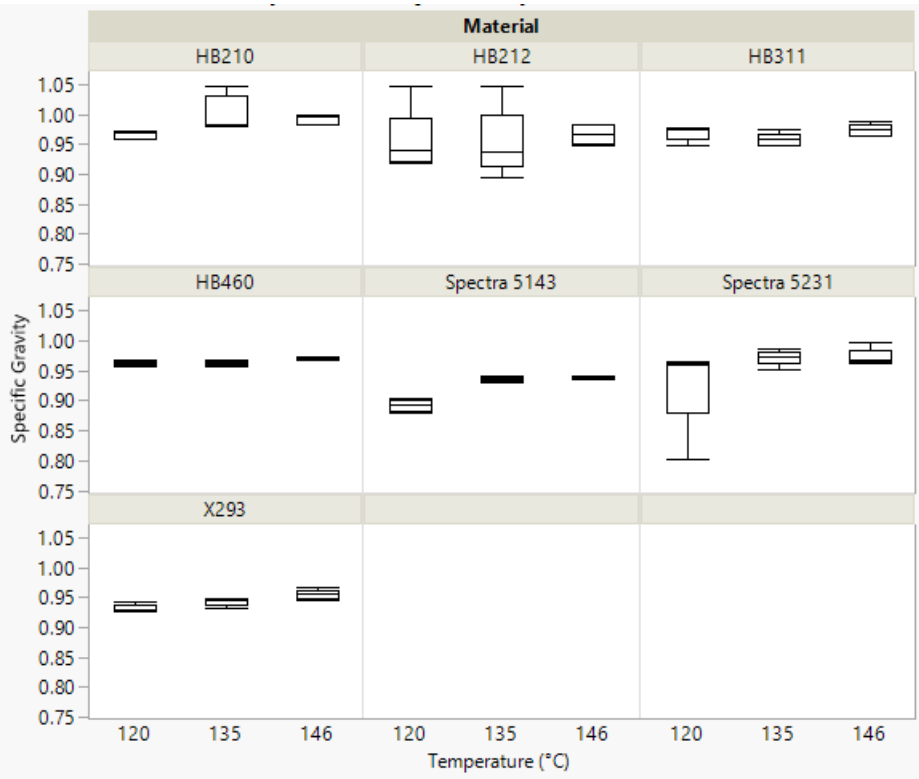

Figure 2 - Specific gravity vs processing temperature for composites processed at 20.7 MPa (3000 psi)

A comparison of means showed that there was a statistically significant ($p<0.05$) difference in specific gravity for HB460 and X293 samples processed at 146 ˚C (295 ˚F). For Spectra 5143, there was a statistically significant difference for samples processed at 120 ˚C (248 ˚F).

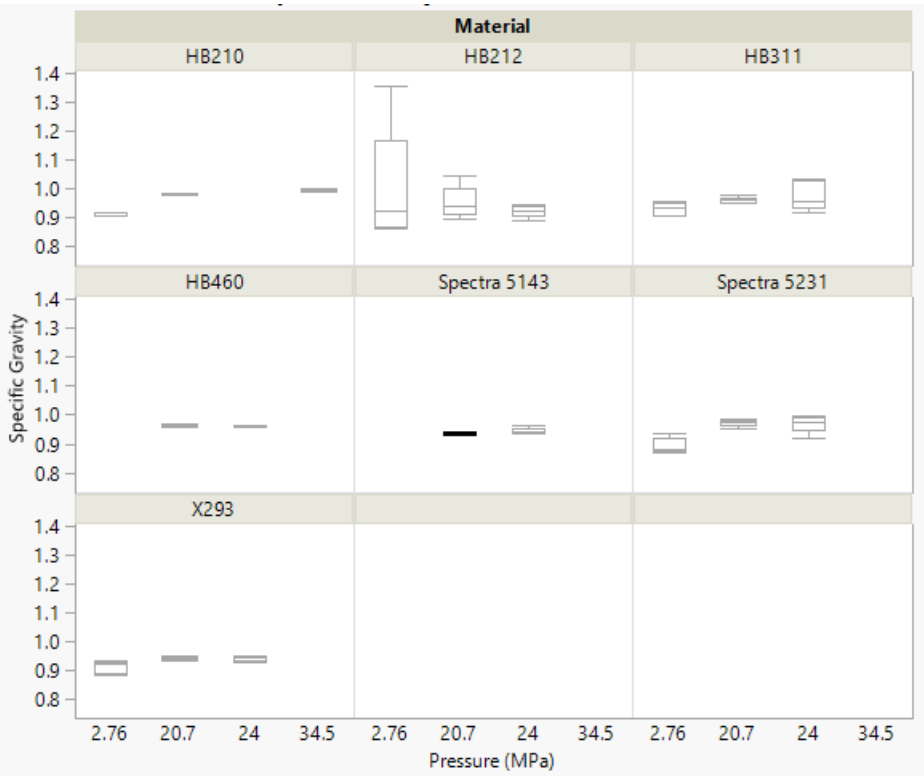

Figure 3 - Specific gravity vs processing pressure for composites processed at 135 ˚C (275 ˚F)

A comparison of means showed that for HB210, Spectra 5231, and X293, there was a statistically significant difference in specific gravity for samples processed at 2.76 MPa (400 psi).

4.2 Micro CT

Figures 5 and 6 show the specific gravity and defect volume ratio as calculated by micro CT scans as functions of processing temperatures and pressures. It is expected that the specific gravity will decrease as porosity increases if the density is indeed changing due to pores in the material. Other factors affecting density include the formation of less-dense amorphous regions if crystalline polymer regions are deformed during processing. This would not be accounted for in the porosity measurements from CT scans. The CT scans may also include areas of the sample affected by method of sample preparation. A first round of samples for image analysis were cut using a band saw, which caused some delamination at the edges, leading to an artificially inflated defect volume ratio. The second round of samples were cut with a water jet to mitigate this issue, but in some materials the water also leads to delamination.

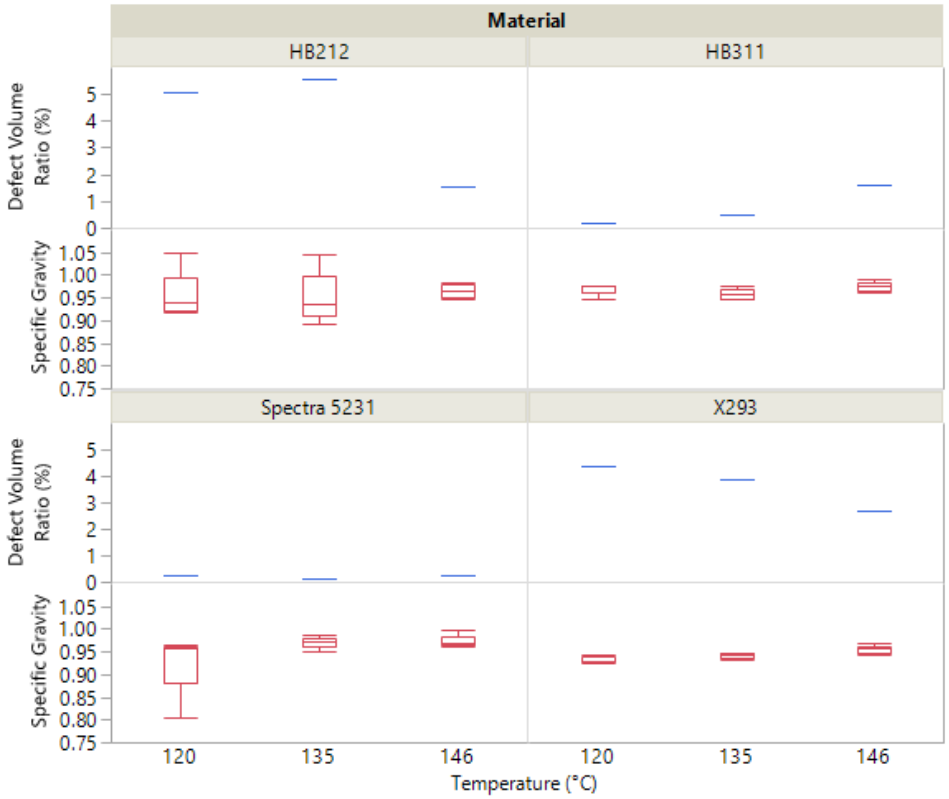

Figure 4 - Specific gravity and defect volume ratio vs processing temperature for composites processed at 20.7 MPa (3000 psi)

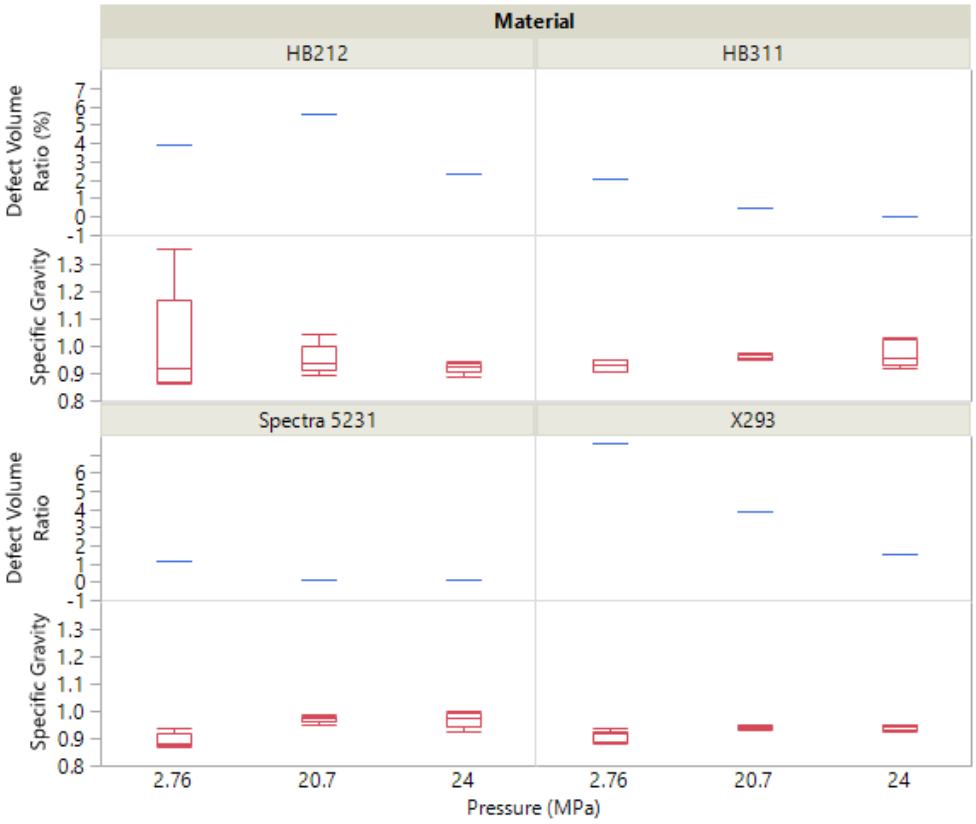

Figure 5 - Specific gravity and defect volume ratio vs processing pressure for composites processed at 135 ˚C (275 ˚F)

An example of a micro CT scan is shown in Figure 7. Figure 7a shows a cross-section of HB311 processed at 2.76 MPa (400 psi) and Figure 7b shows a cross-section of HB311 processed at 24 MPa (3480 psi). Both were processed at a temperature of 135 ˚C (275 ˚F). The blue indicates areas of empty volume, caused either by delamination from sample preparation or the presence of pores. The sample processed at the lower pressure has increased porosity and decreased density, suggesting that for this material the imperfections are most likely due to pores left by processing.

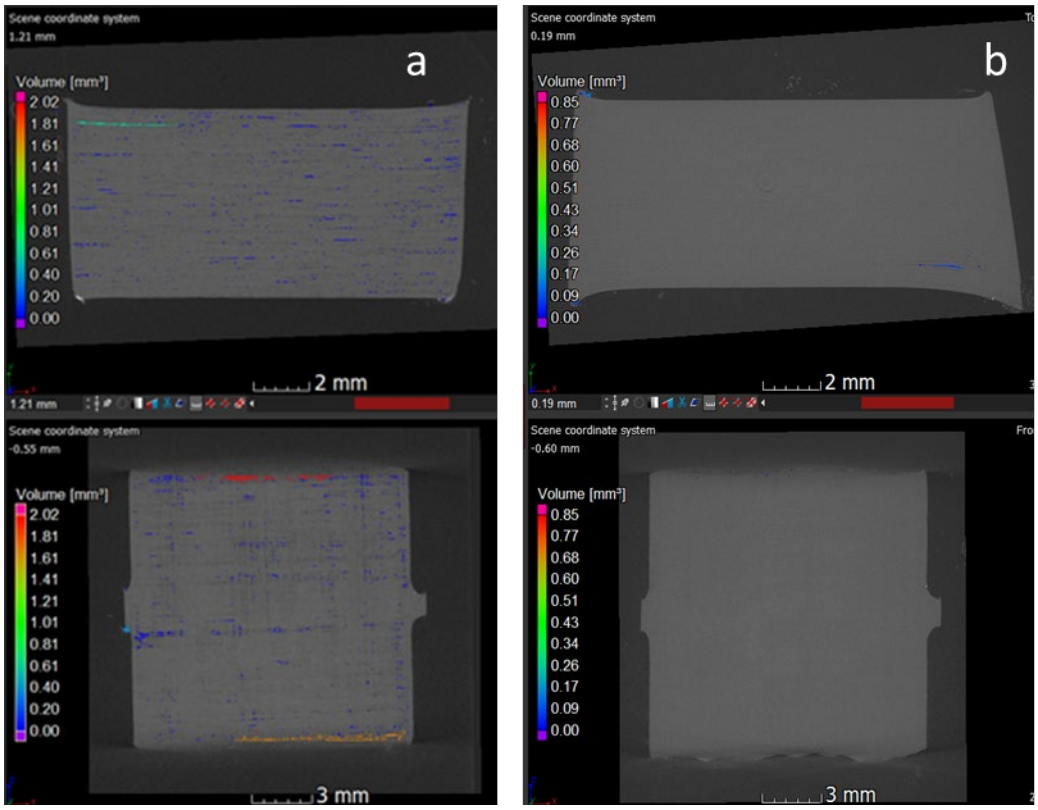

Figure 6 - Micro CT scans of HB311 processed at 135 ˚C and a) 2.76 MPa (400 psi) and b) 24 MPa (3480 psi)

Micro CT may be helpful for qualitative analysis of the material microstructure and at a very small scale could give insights into how pore size and interlaminar structure affect failure mechanisms. However, due to the material sensitivity to preparation methods, density measurements on larger sample sizes are most likely a more accurate quantitative measure of porosity.

4.3 Tensile Strength

Figures 8 and 9 show the effect of processing temperature and pressure on the ultimate tensile strength (UTS) of a strip of one lamina of composite material. It is assumed that the matrix and horizontal fibers do not contribute to the strength of the material. This test is used as an indicator of how the fiber in the composite is affected by processing conditions.

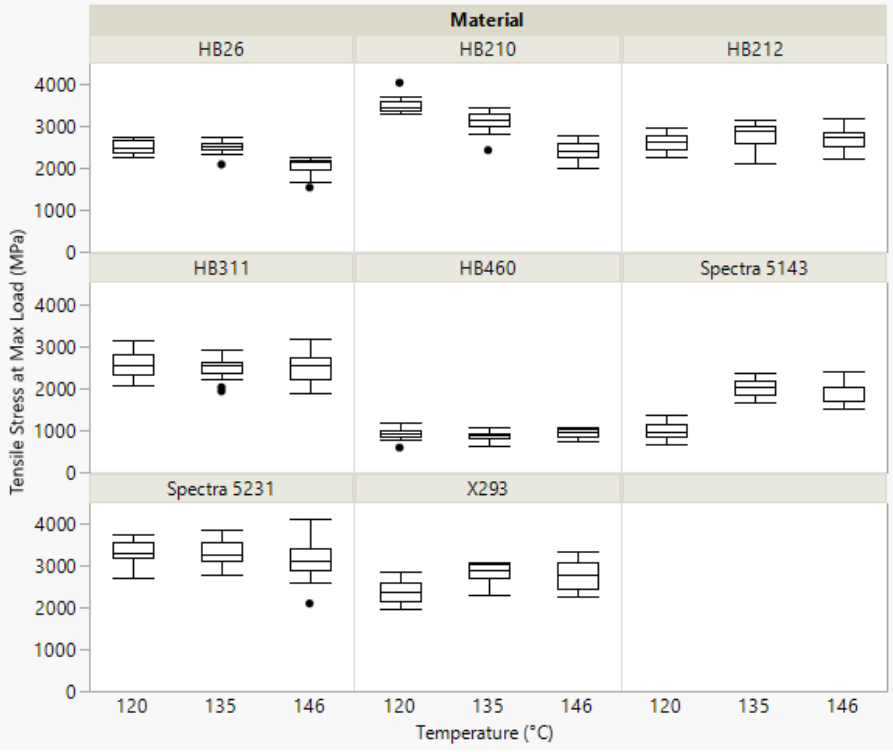

Figure 7 - Ultimate tensile strength vs processing temperature for composites processed at 20.7 MPa (3000 psi)

Comparison of means showed that for HB26, there was a statistically significant difference in tensile strength for samples processed at 146 ˚C (295 ˚F). HB210 samples showed statistically significant differences in tensile strength at all processing temperatures. Spectra 5143 and X293 samples processed at 120 ˚C (248 ˚F) showed a significant decrease in tensile strength.

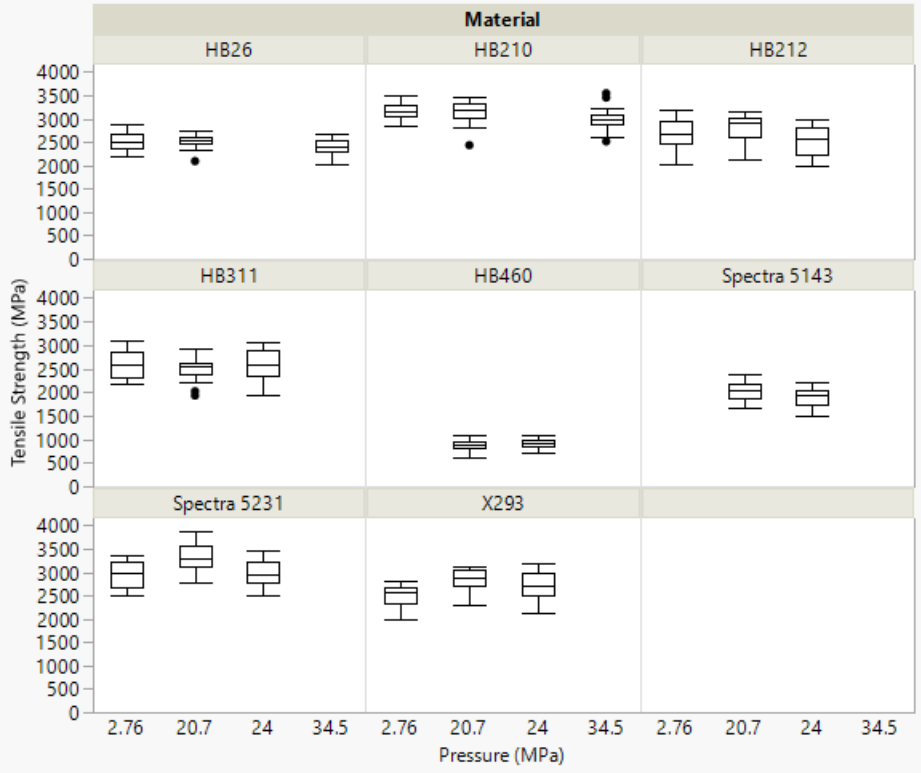

Figure 8 - Ultimate tensile strength vs processing pressure for composites processed at 135 ˚C (275 ˚F)

There was a statistically significant difference in tensile strength between HB26 and HB210 processed at 2.76 MPa (400 psi) as compared to 34.5 MPa (5000 psi). For HB212 there was a significant difference between samples processed at 20.7 MPa (3000 psi) as compared to 24 MPa (3480 psi). Spectra 5231 showed a statistically significant difference in tensile strength for samples processed at 20.7 MPa (3000 psi) as compared to the other two pressure conditions. X293 showed a significant decrease in tensile strength for samples processed at the low pressure of 2.76 MPa (400 psi).

4.4 Short Beam Shear Strength

Figures 10 and 11 show the effect of processing conditions on the short beam shear (SBS) strength of composites using a three-point bend method.

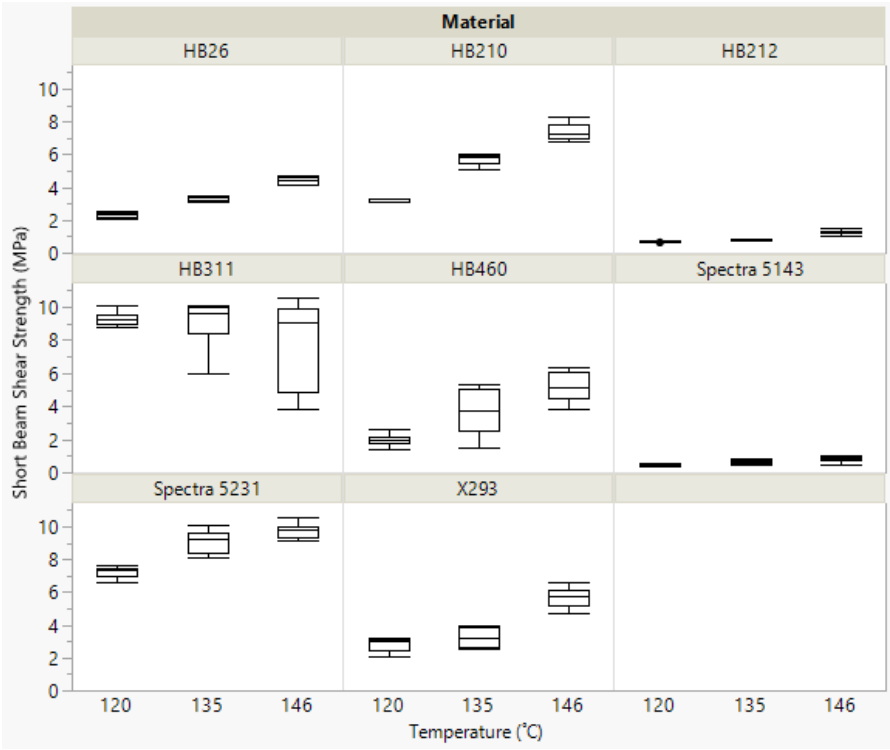

Figure 9 - SBS strength vs processing temperature for composites processed at 20.7 MPa (3000 psi)

Comparison of means showed statistically significant differences in SBS strength between all processing temperatures for HB26, HB210, HB212, HB460, Spectra 5143, and Spectra 5231. X293 showed a significant difference for samples processed at 146 ˚C (295 ˚F). Only HB311 did not exhibit temperature sensitivity. The low values exhibited for Spectra 5143 and HB212 can most likely be attributed to the resin type. These two materials contain a pliable rubber-based resin while the other materials contain a stiffer polyurethane resin.

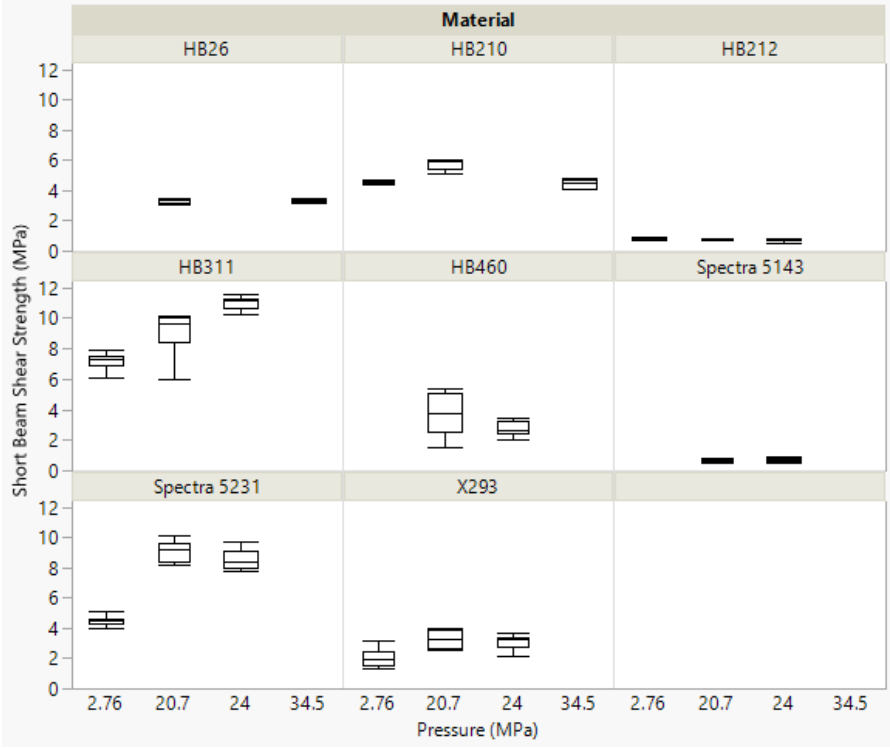

Figure 10 - SBS strength vs processing temperature for composites processed at 135 ˚C (275 ˚F)

Analysis of means showed that for HB210 there was a statistically significant difference in SBS strength for samples processed at 20.7 MPa (3000 psi) as compared to those processed at 2.76 MPa (400 psi) and 34.5 MPa (3480 psi). There was a significant difference in strength for HB212 samples processed at 2.76 MPa (400 psi) as compared to 24 MPa (3480 psi). HB311 showed significant differences between all processing conditions. HB460 showed a significant decrease in SBS strength for samples processed at 24 MPa (3480 psi) as compared to 20.7 MPa (3000 psi). Spectra 5231 and X293 showed a statistically significant decrease in SBS strength for samples processed at 2.76 MPa (400 psi).

4.5 Flexural Strength

Figures 12 and 13 show the effect of processing conditions on the flexural strength of composites using a four-point bend method.

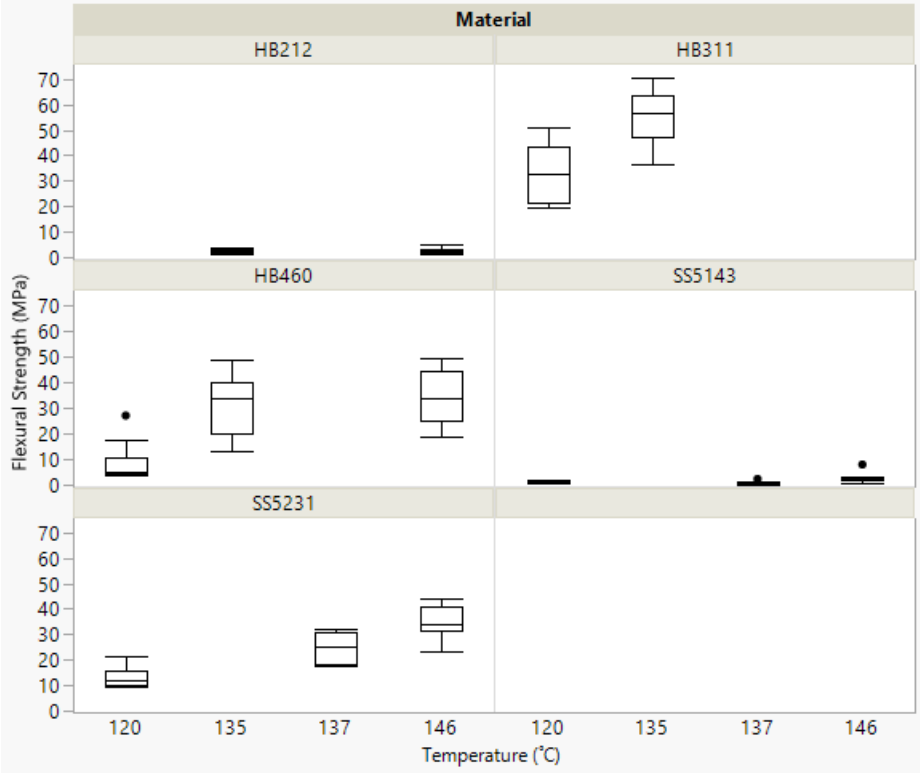

Figure 11 - Flexural strength vs processing temperature for composites processed at 20.7 MPa (3000 psi)

HB311 showed a statistically significant increase in flexural strength for samples processed at 135 ˚C (275 ˚F) as compared to those processed at 120 ˚C (248 ˚F). HB460 samples processed at 120 ˚C (248 ˚F) had a significantly lower flexural strength than samples processed at higher temperatures. Spectra 5143 showed a significant difference between samples processed at 146 ˚C (295 ˚F) and 137 ˚C (275 ˚F). Spectra 5231 had significant differences in flexural strength between all processing temperatures.

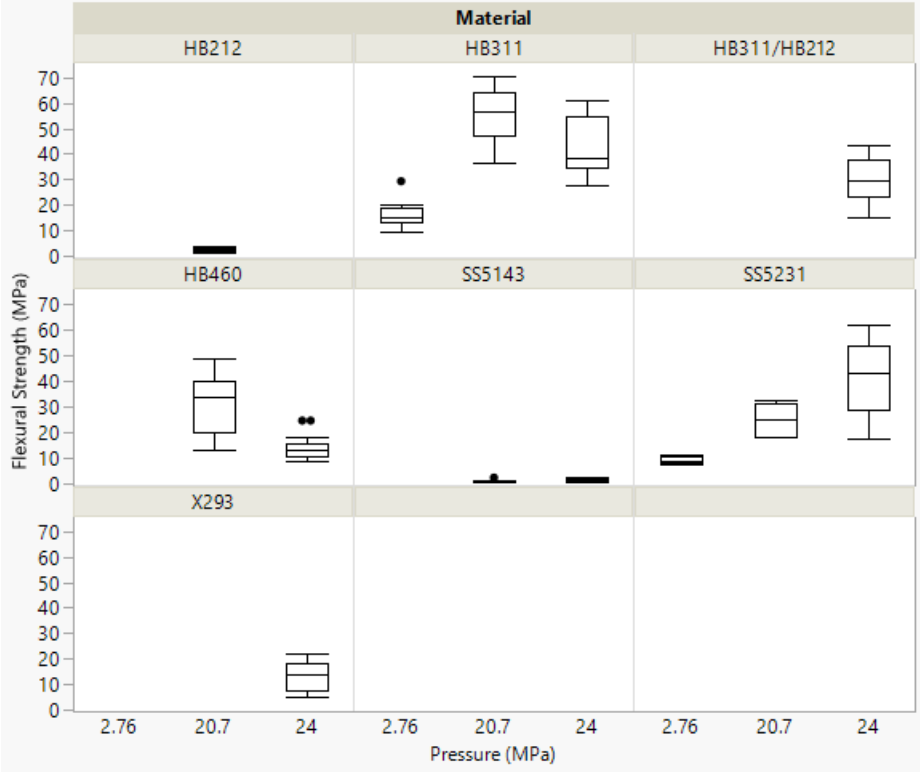

Figure 12 - Flexural strength vs processing temperature for composites processed at 135 ˚C (275 ˚F)

A comparison of means showed that HB311, HB460, and Spectra 5231 had statistically significant differences in flexural strength between all processing pressures.

4.6 Ballistic Tests

Figures 14 and 15 show the V_{50} velocities obtained for composites and composite/ceramic samples tested against 1.1 g (17 gr) FSPs, 2.85 g (44 gr) FSPs, and Threat E. Due to cost constraints, only one processing condition for each material was selected for Threat E ballistic testing.

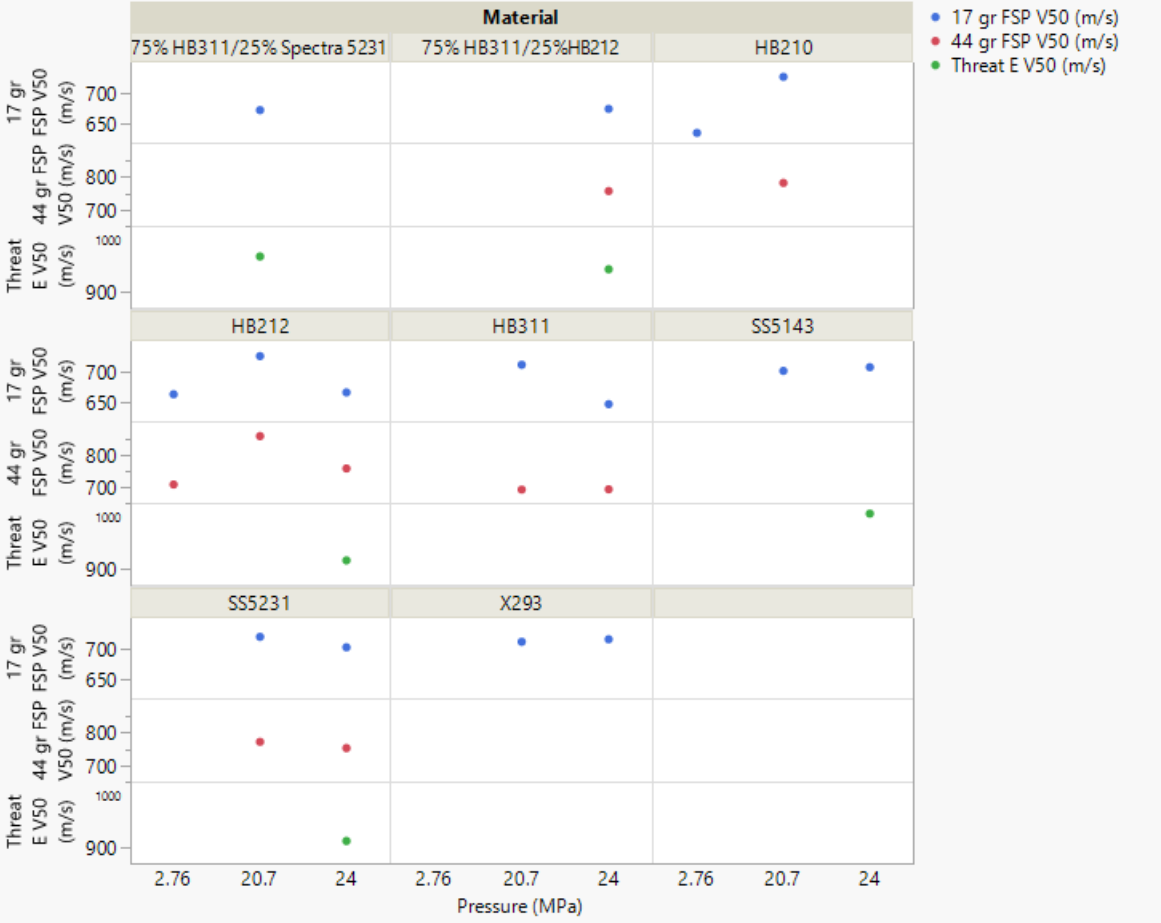

Figure 13 - V_{50} for 1.1 g (17 gr) FSP, 2.85 g (44 gr) FSP, and Threat E vs processing temperature for composites processed at 20.7 MPa (3000 psi)

It can be concluded that HB210, HB212, and HB311 showed significant (ΔV_{50} > ~ 60 m/s (200 ft/s)) improvement in V_{50} FSP protection when processed at 20.7 MPa (3000 psi). Performance decreased at higher processing pressures.

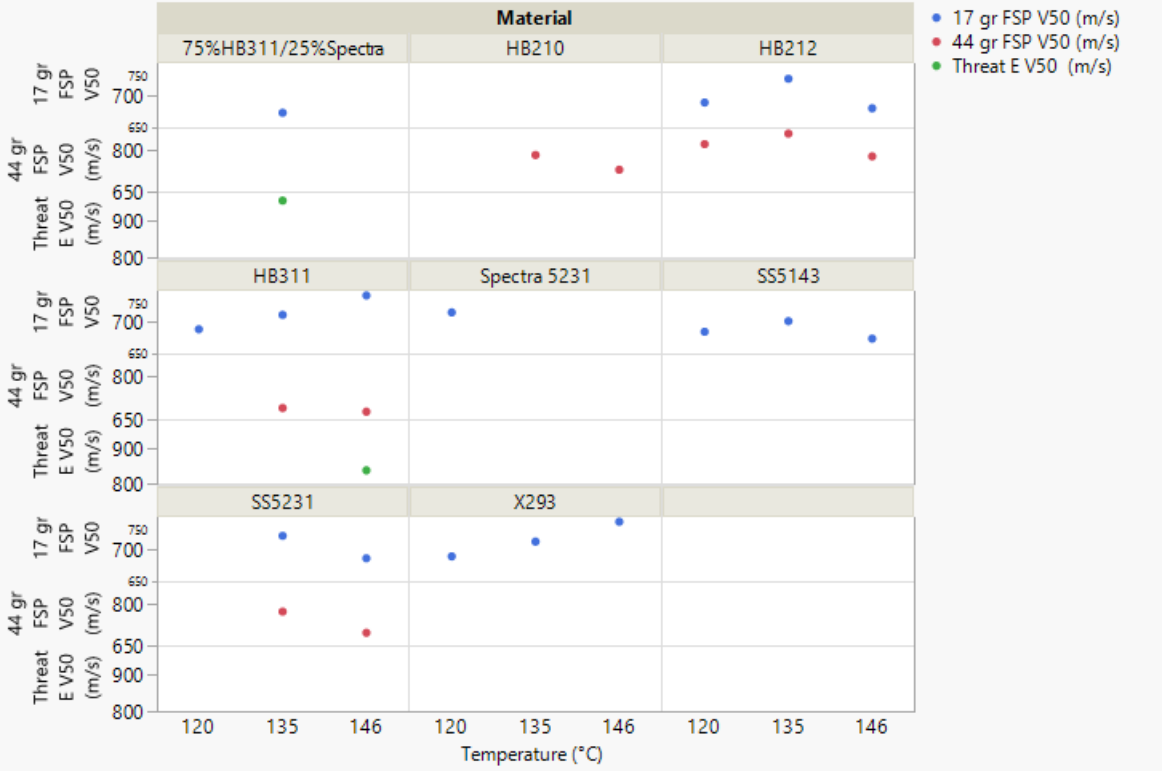

Figure 14 - V50 for 1.1 g (17 gr) FSP, 2.85 g (44 gr) FSP, and Threat E vs processing pressure for composites processed at 135 ˚C (275 ˚F)

X293 showed a significant increase in performance between the low and high processing temperatures for 1.1 g (17 gr) FSP protection, but processing temperature did not otherwise seem to affect ballistic protection.

The mechanical property and FSP testing can be performed in-house at CCDC SC on a relatively small sample size. For this reason, it would be beneficial to be able to relate these properties to the V_{50} performance of an armor system against Threat E, which must be tested at an independent facility with a large number of samples and additional testing costs. Several methods of analysis were used to determine if any of the in-house lab measurements could be used as ballistic performance predictors.

A response screening analysis using JMP® software uses a linear regression method of comparing sets of continuous variables. As shown in Table 5, there were no statistically significant ($p<0.05$) predictors for the Threat E V_{50}, although flexural strength was the strongest predictor with $p=0.055$.

Table 5 - p-values for predictor variables given by response screening analysis

Predictor	P value
Flexural Strength	0.055
SBS Strength	0.23
1.1 g (17 gr) FSP V_{50}	0.40
Specific Gravity	0.41
Tensile Strength	0.66

Predictor screening was also used to determine which variables, if any, can be used to predict a Threat E V_{50}. Unlike with response screening, which tests factors one at a time, predictor screening uses a bootstrap forest partitioning method. The partition model can evaluate predictors singularly or in combination with other predictors. Table 6 shows the results of this model, which ranks each variable according to their contribution. As with the response screening model, flexural strength was the highest predictor for Threat E V_{50} performance.

Table 6 - Predictor screening analysis of predictor variables for Threat E V_{50}

Predictor	Contribution portion	Rank
Flexural Strength	0.29	1
1.1 g (17 gr) FSP V_{50}	0.22	2
SBS Strength	0.21	3
Specific Gravity	0.19	4
Tensile Strength	0.09	5

Similar to the response screening method, a generalized linear fit regression model was used to screen each predictor individually. The whole model test gives the probability of obtaining a greater χ^2 value if the regression model fits no better than a model containing only an intercept. χ^2 is a measure of goodness of fit. If the probability p is <0.05, then the model is considered significant. These values are shown for each predictor variable in Table 7. In agreement with the response and predictor screening methods, only the flexural strength was a good predictor of Threat E performance.

Table 7 - p-values for predictor variables given by a generalized linear fit regression model

Predictor	P, model significance
Flexural Strength	0.013
SBS Strength	0.0955
1.1 g (17 gr) FSP V_{50}	0.2431
Specific Gravity	0.2563
Tensile Strength	0.5408

A multivariate matrix shown in Figure 16 gives a visual representation of each variable in relation to one another. This also confirms that Threat E protection and flexural strength have a negative correlation.

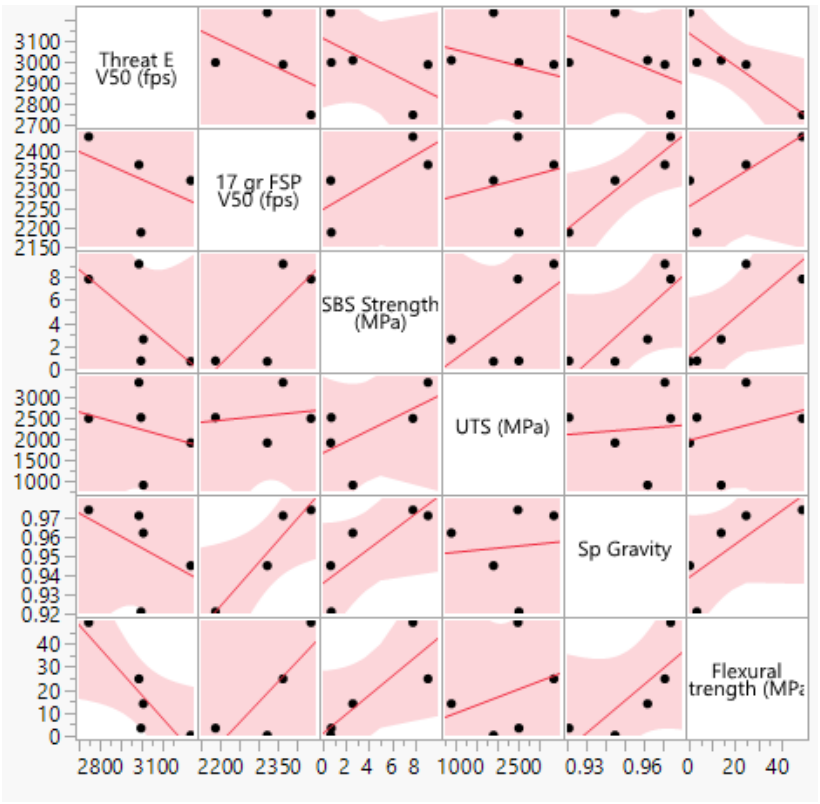

Figure 15 - Scatterplot matrix for all performance variables

While the different screening methods are all in agreement with each other, it should be noted that each of these statistical methods is meant for large data sets. For this data set, where n=6, the models may be over- or under-fitting the data.

5 Conclusions

The overall goal of this project was to relate ballistic performance of ceramic/composite armor systems against Threat E to a test which is easily performed at the lab bench scale. Statistical analysis showed that the best predictor of Threat E protection is the flexural strength of the composite backing material.

Figures 11 and 12 show that the flexural strength can be optimized for certain composite materials by tuning the processing conditions.

Future work should include ballistic testing against other relevant threats to determine if mechanical properties of a composite can be related to other threats in the same way it can for Threat E.

This document reports research undertaken at the U.S. Army Combat Capabilities Development Command Soldier Center, Natick, MA, and has been assigned No. Natick/TR-22/032 in a series of reports approved for publication

6 References

[1] ASTM Standard D792-13, 2013, “Standard Test Methods for Density and Specific Gravity (Relative Density) of Plastics by Displacement,” ASTM International, West Conshohocken, PA.

[2] ASTM Standard D2344M-13, 2013, “Standard Test Method for Short-Beam Strength of Polymer Matrix Composite Materials and Their Laminates,” ASTM International, West Conshohocken, PA.

[3] Ghiorse, S.; Horwath, E., Montgomery, J.; and Hoppel, C. “Effect of Backing Plate Properties on the Ballistic Response of Ceramic-Based Structural Armor.” ARL-RP-56. Sept 2002.

[4] ASTM Standard D7264, 2015, “Standard Test Method for Flexural Properties of Polymer Matrix Composite Materials,” ASTM International, West Conshohocken, PA.

Appendix

Material	Pressure MPa (psi)	Temperature °C (°F)
Dyneema® HB210	20.7 (3000)	135 (275)
	2.76 (400)	135 (275)
	34.5 (5000)	135 (275)
	20.7 (3000)	146 (295)
Dyneema® HB212	20.7 (3000)	135 (275)
	2.76 (400)	135 (275)
	24.0 (3480)	135 (275)
	20.7 (3000)	146 (295)
	20.7 (3000)	120 (248)
Dyneema® HB311	20.7 (3000)	135 (275)
	24.0 (3480)	135 (275)
	20.7 (3000)	146 (295)
	20.7 (3000)	120 (248)
Dyneema® HB460	20.7 (3000)	135 (275)
	24.0 (3480)	135 (275)
	20.7 (3000)	146 (295)
	20.7 (3000)	120 (248)
Dyneema® X293	20.7 (3000)	135 (275)
	2.76 (400)	135 (275)
	24.0 (3480)	135 (275)
	20.7 (3000)	146 (295)
	20.7 (3000)	120 (248)
Spectra Shield® 5143	20.7 (3000)	135 (275)
	24.0 (3480)	135 (275)
	20.7 (3000)	146 (295)
	20.7 (3000)	120 (248)
Spectra Shield® 5231	20.7 (3000)	135 (275)
	24.0 (3480)	135 (275)
	20.7 (3000)	146 (295)
	20.7 (3000)	120 (248)
Dyneema® HB311/HB212	24.0 (3480)	135 (275)
Dyneema® HB311/Spectra Shield® 5231	24.0 (3480)	135 (275)